nearest neighbors. The equilibrium equations can be derived as in Refs. 3 and 6 and involve a force balance between the fiber in question and the shear force induced by the relative axial displacement of the given fiber and the nearest neighboring fibers via the matrix shear strain. For the *HM* fibers, they are

$$\frac{d^2U_{n,m}}{d\xi^2} + U^*_{n+1,m} + U^*_{n,m+1} + U^*_{n-1,m} + U^*_{n,m-1} - 4U_{n,m} = 0 \tag{10}$$

For *LM* fibers, we get

$$\frac{Rd^2U^*_{n,m}}{d\xi^2} + U_{n+1,m} + U_{n,m+1} + U_{n-1,m} + U_{n,m-1} - 4U^*_{n,m} = 0 \tag{11}$$

Since we deal with finite-width dimensions, additional equations are written[6] for corner and edge fibers. The nondimensional loads are

$$P_{n,m} = U'_{n,m}, \qquad P^*_{n,m} = RU^{*'}_{n,m} \tag{12}$$

and the boundary conditions are the same as in Eqs. (8). For instance, for *HM* fibers, we have

$$P_{n,m}(0) = 0 \ (n,m) \text{ broken}; \ U_{n,m}(0) = 0 \ (n,m) \text{ intact}; \ P_{n,m}(\infty) = 1 \tag{13}$$

The band matrix L in Eq. (7) is now wider, and stress concentration factors (SCF) are calculated in the first unbroken fibers on the major diameter adjacent to the broken fibers. The way in which broken fibers were chosen is the same as in Ref. 3 and is shown in Fig. 1. The number N in Figs. 1 and 3 represents the number of broken fibers on the major diameter and all fibers within a circle of diameter Nd were broken. This approach is motivated for nonhybrids in Ref. 3, where the ratio of the three-dimensional to the two-dimensional SCF is shown to approach the limit $2/\pi$ as N gets very large. This limit is shown to be the same as the corresponding ratio, for the continuous problem, of the three-dimensional SCF as the edge of a disk-shaped void in a three-dimensional body is approached to the two-dimensional SCF as the edge of a crack in a sheet is approached.

Results and Discussion

Results for the stress concentration factor (SCF) in the first unbroken fiber adjacent to a series of fiber breaks are shown in Figs. 2 and 3. In the two-dimensional case, the SCF for an *HM* fiber is equal to the value of P_n in the first unbroken *HM* fiber. For the first unbroken *LM* fiber, it is equal to P^*_n/R. A similar approach is used in the three-dimensional case. Figure 2 plots the SCF against the parameter R for various values of continuous breaks r. In this two-dimensional model, there is a total of 25 fibers. While the SCF increases for the *LM* fibers, it decreases for the *HM* fibers as R goes from 1 to 0.2. This indicates partly how, for smaller values of R, which imply a greater difference in the axial stiffness of the alternating fibers, a greater hybrid effect can be realized. In Fig. 3, the SCF is plotted against R for the three-dimensional model. The number of continuous fiber breaks on the major diameter (see Fig. 1) is given by N, and there is a total of 225 fibers. It is apparent that the SCF for the three-dimensional model is not only less than that for the model, but the two-dimensional model SCF is also more sensitive to R, with greater increases in SCF for *LM* fibers and greater decreases in SCF for *HM* fibers as R goes from 1 to 0.2.

References

[1]Fukuda, H., and Chou, T. W., "Stress Concentrations in a Hybrid Composite Sheet," *ASME Journal of Applied Mechanics*, Vol. 50, Dec. 1983, pp. 845-848.

[2]Hedgepeth, J. M., "Stress Concentrations in Filamentary Structures," NASA TN D-882, 1961.

[3]Hedgepeth, J. M., and Van Dyke, P., "Local Stress Concentrations in Imperfect Filamentary Composite Materials," *Journal of Composite Materials*, Vol. 1, April 1967, pp. 294-309.

[4]Rossettos, J. N., and Shishesaz, M., "Stress Concentration in Fiber Composite Sheets Including Matrix Extension," *ASME Journal of Applied Mechanics*, Vol. 54, Sept. 1987, pp. 722-724.

[5]Strang, G., *Linear Algebra and Its Applications*, Academic, New York, 1980.

[6]Sakkas, K., "Stress Analysis in Hybrid Composites Using the Shear Lag Model," Thesis, Dept. of Mechanical Engineering, Northeastern Univ., Boston, MA, 1986.

Differentia' Equation Based Method for Accurate Modal Approximations

Jocelyn I. Pritchard* and Howard M. Adelman†
Langley Research Center, Hampton, Virginia 23665

Introduction

IT is highly desirable in optimization to be able to calculate the effect of design variable changes without having to perform a full analysis for each design iteration. This need has led to an increased interest in accurate and efficient approximation techniques. Many optimization procedures use first-order Taylor series approximations of the objective function and constraints for this purpose.[1] Taylor series and other approximations are also used outside of optimization for quick assessments of the effect of design changes.[2-9] In this paper, an efficient method is described that significantly extends the range of applicability of approximations beyond the range of the linear Taylor series approach. The key to the new approach is to recognize that the formulas for the sensitivity derivatives of system behavior variables can be interpreted as differential equations that may be solved to obtain closed form exponential approximations. Herein, these approximations will be referred to as the Differential Equation Based (DEB) approximations.

Basis of DEB Method

The DEB method is exemplified by investigating the sensitivity equations for eigenvalues and eigenvectors. First, the method will be developed for the approximation of vibration frequencies, and then mode shapes.

Approximation of Frequencies

As given in Ref. 10, the equation for the derivative of the vibration eigenvalue ω^2 with respect to a design variable, v is

$$\frac{d\omega^2}{dv} = b - a\omega^2 \tag{1}$$

where

$$a = \Phi^T \frac{dM}{dv} \Phi \qquad b = \Phi^T \frac{dK}{dv} \Phi \tag{2}$$

Received Jan. 19, 1990; revision received April 6, 1990; accepted for publication April 26, 1990.

*Research Engineer, Interdisciplinary Research Office, U.S. Army Aerostructures Directorate.

†Deputy Head, Interdisciplinary Research Office, NASA. Member AIAA.

K is the stiffness matrix, M the mass matrix, and Φ the eigenvector normalized such that $\Phi^T M \Phi = 1$. Equation (1) may be interpreted as a first-order differential equation in ω^2 with variable coefficients. However, if a and b do not vary extensively with v, then they may be evaluated at the nominal design and considered constant. After applying the nominal condition that $\omega^2 = \omega_o^2$ when $v = v_o$, the general solution to Eq. (1), provided a is nonzero, is

$$\omega^2 = \left(\omega_o^2 - \frac{b}{a}\right) e^{-a(v - v_o)} + \frac{b}{a} \tag{3}$$

For the case where $a = 0$, the method produces the linear Taylor series approximation.[5]

Approximation of Mode Shapes

From Ref. 11, the equation for the derivative of the mode shape Φ, with respect to a design variable, is

$$\frac{d\Phi}{dv} = Q + D\Phi \tag{4}$$

where Q satisfies the equation

$$[K - \omega^2 M]Q = \frac{d\omega^2}{dv} M\Phi - \frac{dK}{dv}\Phi + \omega^2 \frac{dM}{dv}\Phi \tag{5}$$

and

$$D = -\Phi^T M Q - \frac{1}{2}\Phi^T \frac{dM}{dv}\Phi \tag{6}$$

Details of calculating Q and D may be found in Ref. 11. Equation (4) is a nonlinear first-order vector differential equation with variable coefficients. In order to solve this equation, D and Q are evaluated at the nominal design and held constant. After applying the nominal condition that $\Phi = \Phi_o$ when $v = v_o$, the solution to Eq. (4) is

$$\Phi = \left(\Phi_o + \frac{1}{D} Q\right) e^{D(v - v_o)} - \frac{1}{D} Q \tag{7}$$

Equation (7) is a vector equation, however; it is uncoupled in the sense that each component of Φ varies independently with the design variable v. The difference between components is reflected in the corresponding components of Φ_o and Q.

DEB Method Extended to Multiple Design Variables

The solutions described in Eqs. (3 and 7) are directly applicable only when a single design variable is perturbed. To approximate the effect of simultaneous changes in several design variables, the DEB method is modified as follows. If v_o is the vector of nominal design variables and v is the vector of perturbed design variables, then $v - v_o$ is the direction of the move from the nominal to the perturbed design. Any design along the move direction may be associated with a scalar θ between 0 and 1. Then

$$v(\theta) = v_o + \theta(v - v_o) \tag{8}$$

In particular $v(1) = v$ and $v(0) = v_o$. Now the sensitivity Eqs. (1) and (4) may each be written with θ as the independent variable. For example, Eq. (1) is rewritten as

$$\frac{d\omega^2}{d\theta} = b_\theta - a_\theta \omega^2 \tag{9}$$

where

$$a_\theta = \Phi^T \frac{dM}{d\theta}\Phi \qquad b_\theta = \Phi^T \frac{dK}{d\theta}\Phi \tag{10}$$

$$\frac{dK}{d\theta} = \sum \frac{dK}{dv_i}\frac{dv_i}{d\theta} = \sum \frac{dK}{dv_i}(v_i - v_{oi})$$

$$\frac{dM}{d\theta} = \sum \frac{dM}{dv_i}\frac{dv_i}{d\theta} = \sum \frac{dM}{dv_i}(v_i - v_{oi}) \tag{11}$$

where the index i ranges over the design variables. Then the solution to Eq. (9) is

$$\omega^2(v) = \left(\omega_o^2 - \frac{b_\theta}{a_\theta}\right) e^{-a_\theta s} + \frac{b_\theta}{a_\theta} \tag{12}$$

since $\omega^2(1) = \omega^2(v)$ from Eq. (8) and by definition $\theta_o = 0$. In Eq. (12), s corresponds to the number of steps of length $|v - v_o|$ along the move direction. An extension of the method to multiple design variables has also been developed for Φ.

Results

Approximations for frequencies and mode shapes were implemented and tested. The test cases involved a 193 in. (4.9 m) cantilever box beam (Fig. 1) modeled with 10 equal elements having the following properties: $E = 0.490$ E7 psi (33.8 GPa) for the root element and $E = 0.585$ E7 psi (40.3 GPa) for the remaining elements; $\rho = 0.07$ lb/in.^{3} (1937.6 kg/m^3); the width of the beam $B = 3.75$ in. (9.53 cm); the depth of the beam $H = 5.0$ in. (12.7 cm); the sidewall thickness $d = 0.1$ in. (2.54 mm); and the top and bottom wall thickness $t = 0.8$ in. (2.03 cm). All calculations were generated in Engineering Analysis Language (EAL).[12] The test cases involved perturbations of the height, width, cross-sectional area, tip mass, and bending inertia of the beam. Results were compared with exact solutions and the commonly-used Taylor series approximation.

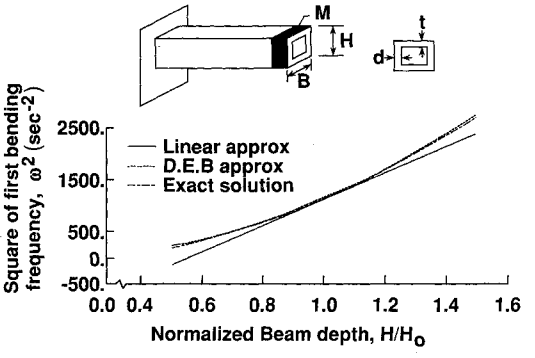

Fig. 1 Comparison of DEB and linear approximations of frequency for perturbation of beam depth H. [$B = 3.75$ in. (9.53 cm), $M = 0$ lbm].

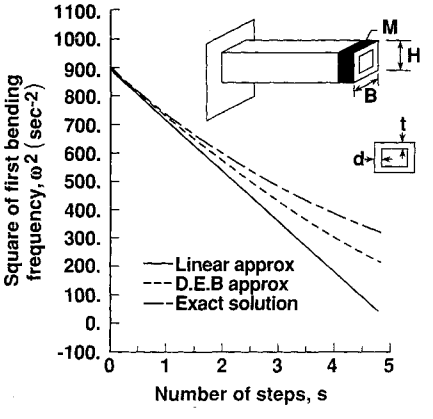

Fig. 2 Comparison of DEB and linear approximations of frequency for simultaneous perturbation of tip mass, bending inertia, and cross-sectional area. (Each step represents 10% perturbation in the design variables from the nominal.)

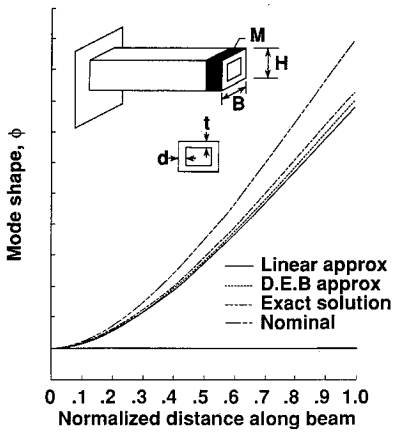

Fig. 3 Comparison of DEB and linear approximations of first bending mode shape for 50% perturbation of beam width *B*. [Nominal values; $H = 5.0$ in. (12.7 cm), $M = 0$ lbm, $B = 3.75$ in. (9.53 cm).]

Figure 1 shows a graph of the fundamental eigenvalue as a function of the height of the beam H for values perturbed from the nominal value (H_o) of 5.0 in. (12.7 cm). For as much as a 50% increase in H, the new approximation is within 2% of the exact solution, compared to 12% for the Taylor series approximation. It is also evident from the figure that, for decreases in H exceeding 45%, the Taylor series method gives negative values for the eigenvalues.

Figure 2 illustrates the application of the DEB method to simultaneous changes in three design variables: tip mass, bending inertia, and cross-sectional area of the beam. The nominal values of the design variables (corresponding to $\theta = 0$) are $M = 5.0$ lbs (2.268 kg), $I = 28.863$ in.^{4} (1201.4 cm^4), and $A = 7.0$ in.^{2} (45.2 cm^2). Perturbations were made in increments of 10% of these nominal values. Results from the DEB approximation were very encouraging, and for even as much as a 50% increase in the design variables there was still only a 32% error compared to nearly a 100% error for the Taylor series approximation. Similar trends occurred for other variables in approximating frequencies of the first and second bending modes.

Figure 3 shows a sketch of the first bending mode shape for the nominal design, the Taylor series approximation, the DEB approximation, and the exact solution for a 50% perturbation in the beam width B. Both approximations are very accurate, but the DEB approximation is closer to the exact curve.

Concluding Remarks

This note has demonstrated that sensitivity equations, when interpreted as differential equations, may be used to generate accurate approximations. To date, the method has been developed and demonstrated for frequency and mode shape approximations. In principle, the method is applicable to approximating any quantity for which an analytical sensitivity formula is available. For example, approximating displacements is a potential extension of this concept.

Acknowledgment

The authors wish to express their special thanks to Raphael T. Haftka of Virginia Polytechnic Institute and State University for his valuable discussions and suggestions during the course of this research.

References

[1]Walsh, J. L., "Application of Mathematical Optimization Procedures to a Structural Model of a Large Finite-Element Wing," NASA TM-87597, Jan. 1986.

[2]Storaasli, O. O., and Sobieszczanski, J., "On the Accuracy of the Taylor Approximation for Structure Resizing," *AIAA Journal,* Vol. 12, Feb. 1974, pp. 231–233.

[3]Haftka, R. T., and Shore, C. P., "Approximate Methods for Combined Thermal Structural Design," NASA TP-1428, 1979.

[4]Vanderplaats, G. N., and Salajegheh, E., "New Approximation Method for Stress Constraints in Structural Synthesis," *AIAA Journal,* Vol. 27, No. 3, 1989, pp. 352–358.

[5]Schmit, L. A., and Farshi, B., "Some Approximation Concepts for Structural Synthesis," *AIAA Journal,* Vol. 12, No. 5, 1974, pp. 692–699.

[6]Prasad, B., "Potential Forms of Explicit Constraint Approximations in Structural Optimization—Part 1: Analysis and Projections," *Computer Methods in Applied Mechanics and Engineering,* Vol. 40, No. 1, 1983, pp. 245–261.

[7]Inamura, T., "Eigenvalue Reanalysis by Improved Perturbation," *International Journal for Numerical Methods in Engineering,* Vol. 26, Jan. 1988, pp. 167–181.

[8]Miura, H., and Schmit, L. A., "Second Order Approximation of Natural Frequency Constraints in Structural Synthesis," *International Journal for Numerical Methods in Engineering,* Vol. 13, No. 2, 1978, pp. 337–351.

[9]Wang, B. P., and Pilkey, W. D., "Eigenvalue Reanalysis of Locally Modified Structures Using a Generalized Rayleigh's Method," *AIAA Journal,* Vol. 24, June 1986, pp. 983–990.

[10]Fox, R. L., and Kapoor, M. P., "Rate of Change of Eigenvalues and Eigenvectors," *AIAA Journal,* Vol. 6, Dec. 1968, pp. 2426–2429.

[11]Nelson, R. B., "Simplified Calculation of Eigenvector Derivatives," *AIAA Journal,* Vol. 14, No. 9, 1976, pp. 1201–1205.

[12]Whetstone, W. D., *Engineering Analysis Language Reference Manual-EISI-EAL System Level 2091,* Engineering Information Systems, Inc. EISI-EAL, San Jose, CA, July 1983.

Three-Dimensional Shape Optimization with Substructuring

M. E. Botkin* and R. J. Yang†
General Motors Research Laboratories, Warren, Michigan 48090

Introduction

PREVIOUS research on shape optimization has been focused on design sensitivity theory,[1,2] and design modeling techniques,[2–7] with usually the entire structure being analyzed and subsequently optimized. In a real design environment, one often encounters the fact that only a small part of a complicated component is allowed to change. In this case, substructure analysis is a more efficient approach than the full-structure finite element approach in an iterative design process. Since, especially in structural optimization, the structure has to be analyzed for each design iteration, the substructure approach is a very efficient tool for a large problem.[8] In shape optimization, the computational advantage is not only in analysis but also in the sensitivity calculations. The CPU reduction in analysis and the sensitivity calculations result in a more efficient optimization process.

Substructure Analysis

The substructure concept is, first, to divide the complete structure into several regions, condense the interior degrees of freedom to the boundaries of the regions, and then establish

Presented as Paper 89-1221 at the AIAA/ASME/ASCE/AHS/ASC 30th Structures, Structural Dynamics, and Materials Conference, Mobile, AL, April 3–5, 1989; received April 17, 1989; revision received and accepted for publication April 17, 1990.

*Senior Staff Research Engineer, Engineering Mechanics Department.

†Principal Research Engineer, Engineering Mechanics Department; currently at Ford Scientific Research Laboratory, Dearborn, Michigan.